

Modulational instabilities in discrete lattices

Yuri S. Kivshar*

Institut für Theoretische Physik I, Heinrich-Heine Universität Düsseldorf, D-4000 Düsseldorf 1, Germany

Michel Peyrard

*Physique Non Linéaire, Ondes et Structures Cohérentes, Faculté des Sciences, 6 boulevard Gabriel, F-21000 Dijon, France
and Center for Nonlinear Studies, MS B258, Los Alamos National Laboratory, Los Alamos, New Mexico 87545*

(Received 7 April 1992)

We study analytically and numerically modulational instabilities in discrete nonlinear chains, taking the discrete Klein-Gordon model as an example. We show that discreteness can drastically change the conditions for modulational instability; e.g., at small wave numbers a nonlinear carrier wave is unstable to all possible modulations of its amplitude if the wave amplitude exceeds a certain threshold value. Numerical simulations show the validity of the analytical approach for the initial stage of the time evolution, provided that the harmonics generated by the nonlinear terms are considered. The long-term evolution exhibits chaoticlike states.

PACS number(s): 05.45.+b, 03.40.Kf

I. INTRODUCTION

Many nonlinear physical systems exhibit an instability that leads to a self-induced modulation of the steady state as a result of an interplay between the nonlinear and dispersive effects. This phenomenon, referred to as modulational instability, has been studied in such diverse fields as fluid dynamics [1,2], nonlinear optics, [3–5] and plasma physics [6,7]. For instance, in optical fibers, modulational instability requires an anomalous group-velocity dispersion and manifests itself as a breakup of a continuous wave into a train of ultrashort pulses, which has been recently observed experimentally [8,9]. In the above-mentioned contexts, modulational instability appears in continuum models, but it has been recently suggested that it could be responsible for energy-localization mechanisms leading to the formation of large-amplitude nonlinear excitations in hydrogen-bonded crystals or deoxyribonucleic acid (DNA) molecules [10]. These systems are intrinsically discrete and a correct microscopic description involves a set of coupled ordinary differential equations instead of a partial-differential equation. In the strong-coupling limit, discreteness effects are neglected and the phenomenon of nonlinear wave modulation is described by the nonlinear Schrödinger (NLS) equation for the wave envelope, obtained with the assumption that both the carrier wave and the envelope can be treated in the continuum approximation [11,12]. An extension of this approach to cover lattice models is the so-called semidiscrete approximation [13–16] in which the discreteness of the carrier wave is treated explicitly while the envelope is still described in the continuum approximation.

However, in some systems, it is important to treat discreteness completely, i.e., to consider the case where both the carrier wave and the envelope cannot be described in terms of long-wavelength components. This is, for instance, the case for the “breathing modes” of DNA which extend over only one or two base pairs [17]. In

nonlinear lattices, discreteness effects can give rise to intrinsic localized vibrational states [18–20] that would not exist in a continuum system and may be considered a discrete version of soliton excitations in nonintegrable models [21,22]. Modulational instability is a possible mechanism for the generation of such localized states, and, indeed, in this case, discreteness effects must not be ignored in analyzing this phenomenon. In the present paper, we discuss modulational instability in lattice models, taking the Klein-Gordon chain as an example. We derive a discrete NLS equation for the amplitude of the carrier wave and analyze the stability condition of the carrier wave in the lattice. In particular, we show that, above a certain threshold in the wave amplitude, a carrier wave at small wave numbers is unstable to all possible modulations. The validity of this analysis is then checked by numerical simulations that reveal some additional features of modulational instability in discrete systems.

II. ANALYTICAL RESULTS

We consider the dynamics of a one-dimensional chain made of atoms with unit mass, harmonically coupled to their nearest neighbors and subjected to a nonlinear symmetric on-site potential. Denoting by $u_n(t)$ the displacement of atom n , its equation of motion is

$$\ddot{u}_n = K(u_{n+1} + u_{n-1} - 2u_n) - \omega_0^2 u_n + \beta u_n^3, \quad (1)$$

where K is the coupling constant, ω_0 the frequency of small-amplitude on-site vibrations in the substrate potential, and β the anharmonicity parameter of the potential. Linear oscillations of the chain of frequency ω and wave number q are described by the dispersion relation

$$\omega^2 = \omega_0^2 + 4K \sin^2(q/2), \quad (2)$$

where the lattice spacing has been taken as equal to unity. As shown by Eq. (2), the linear spectrum has a gap ω_0 and is limited by the cutoff frequency $\omega_{\max}^2 = \omega_0^2 + 4K$ due

to discreteness.

Looking for the slow modulation of a carrier wave that has its frequency in the linear frequency band, we substitute into Eq. (1) the trial solution

$$u_n(t) = \phi_n(t)e^{-i\omega_0 t} + \phi_n^*(t)e^{+i\omega_0 t}, \quad (3)$$

where $\phi_n(t)$ is assumed to vary slowly in time with respect to the main oscillation at frequency ω_0 , i.e., $\dot{\phi}_n \ll \omega_0 \phi_n$. Using the so-called "rotating-wave" approximation, i.e., keeping only the terms proportional to $\exp(\pm i\omega_0 t)$, we obtain a discrete NLS equation for the complex function $\phi_n(t)$,

$$2i\omega_0 \dot{\phi}_n + K(\phi_{n+1} + \phi_{n-1} - 2\phi_n) + 3\beta|\phi_n|^2 \phi_n = 0. \quad (4)$$

The assumption of the slow variation of ϕ_n as well as the neglect of higher-order harmonics to derive Eq. (4) assume that the gap frequency ω_0 is large with respect to the other frequencies in the system, i.e., $\omega_0^2 \gg 4K$ and $\omega_0^2 \gg \beta\phi_0^2$, ϕ_0 being the wave amplitude. The first condition is valid in a weakly dispersive system where ω_{\max} is close to ω_0 , while the second means that the nonlinearity is weak. These are the usual conditions to get the NLS equation, but in the lattice the condition $\omega_0^2 \gg 4K$ also means that discreteness effects will be strong, pointing out the interest of the discrete instead of continuous version of the NLS equation.

Using Eq. (4), derived in the single-frequency approximation, modulational instability in the lattice can be easily analyzed. Equation (4) has a plane-wave exact solution

$$\phi_n(t) = \phi_0 e^{i\theta_n} \quad \text{with} \quad \theta_n = qn - \Delta\omega t, \quad (5)$$

where the frequency $\Delta\omega$ obeys the nonlinear dispersion relation

$$2\omega_0 \Delta\omega = 4K \sin^2(q/2) - 3\beta\phi_0^2. \quad (6)$$

The linear stability of the solution (5) and (6) can be investigated by looking for a solution of the form

$$\phi_n(t) = (\phi_0 + b_n) e^{i\theta_n + i\psi_n}, \quad (7)$$

where $b_n = b_n(t)$ and $\psi_n = \psi_n(t)$ are assumed to be small in comparison with the parameters of the carrier wave. Substituting Eq. (7) into (4), we obtain the two linear equations

$$2\omega_0 \dot{b}_n + K[(b_{n+1} - b_{n-1}) \sin q + \phi_0(\psi_{n+1} + \psi_{n-1} - 2\psi_n) \cos q] = 0, \quad (8)$$

$$-2\omega_0 \phi_0 \dot{\psi}_n + K[(b_{n+1} + b_{n-1} - 2b_n) \cos q - \phi_0(\psi_{n+1} - \psi_{n-1}) \sin q] + 6\beta\phi_0^2 b_n = 0, \quad (9)$$

which yield the dispersion law

$$\begin{aligned} (\omega_0 \Omega - K \sin Q \sin q)^2 \\ = K \sin^2(Q/2) \cos q [4K \sin^2(Q/2) \cos q - 6\beta\phi_0^2] \end{aligned} \quad (10)$$

for the wave number Q and frequency Ω of the linear modulation waves. In the long-wavelength limit, when

$Q \ll 1$ and $q \ll 1$, Eq. (10) reduces to the usual expression for the continuous NLS equation,

$$(\omega_0 \Omega - KqQ)^2 = \frac{1}{4} KQ^2 (KQ^2 - 6\beta\phi_0^2). \quad (11)$$

Equation (10) determines the condition for the stability of a plane wave with wave number q in the lattice. Contrary to what would be found in the continuum limit [Eq. (11)], the stability depends on q . An instability region appears only if $\beta \cos q > 0$. For a given q , e.g., $q < \pi/2$, a plane wave will be unstable to *any* modulation provided that

$$\phi_0^2 > \phi_{0,\text{cr}}^2 = 2K/3\beta. \quad (12)$$

The result (12) is a direct consequence of the fact that, in a lattice, the wave number is bounded by π . Figures 1 and 2 show the regions of modulational instability in the case $\beta > 0$.

One of the main effects of modulational instability is the creation of localized pulses [4]. This is in agreement with the results presented above, which show that, for $\beta > 0$, the small- q region is unstable. Consequently, nonlinearity can induce the formation of localized modes in the gap of the linear spectrum ($\omega^2 < \omega_0^2$). Such a localized mode can be obtained from the discrete NLS equation (4) following the method of Refs. [18], [19], and [22]. In the

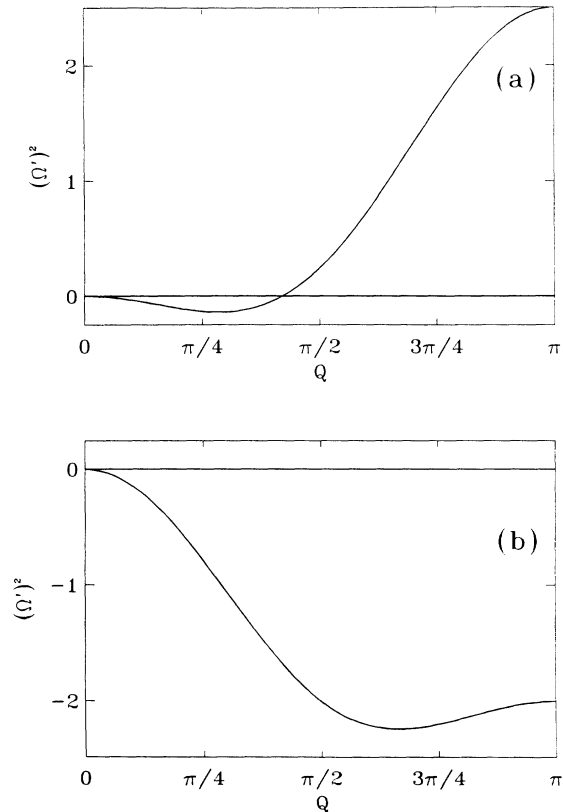


FIG. 1. Variation vs Q of $\Omega^2 = (\omega_0 \Omega - K \sin Q \sin q)^2$ for the modulation waves, for $q=0$ and $\beta > 0$ as the amplitude of the wave crosses the critical value $\phi_{0,\text{cr}}$: (a) $\phi_0^2 < \phi_{0,\text{cr}}^2$ and (b) $\phi_0^2 > \phi_{0,\text{cr}}^2$.

weak-coupling limit $K \ll \beta A^2$, such an excitation

$$\phi_n(t) = A e^{i\Omega t} (\dots, 0, \xi_1, 1, \xi_1, 0, \dots),$$

where the values in the parentheses are the amplitudes at successive sites, and

$$\Omega = -\frac{3\beta}{2\omega_0} A^2, \quad \xi_1 = \frac{K}{3\beta A^2} \ll 1$$

is indeed highly localized. For $\beta > 0$, these nonlinear modes in the chain (1) cannot exist for $\omega^2 > \omega_{\max}^2 = \omega_0^2 + 4K$, because a wave at these frequencies is stable.

It is interesting to compare the results obtained for model (4) with those of the exactly integrable discrete Ablowitz-Ladik equations [23],

$$i\dot{\phi}_n + K'(\phi_{n+1} + \phi_{n-1} - 2\phi_n) + \lambda|\phi_n|^2(\phi_{n+1} + \phi_{n-1}) = 0. \quad (13)$$

Models (4) and (13) (with $K' = K/2\omega_0$) have the same linear properties and lead to the same NLS equation in the continuum limit provided that $\lambda = 3\beta/\omega_0$; however, their nonlinear properties are very different. For model

(13), the dispersion relation for the modulation waves is

$$\begin{aligned} & [\Omega - 2(K' + \lambda\phi_0^2)\sin Q \sin q]^2 \\ &= 16(K' + \lambda\phi_0^2)\sin^2(Q/2)\cos^2 q \\ & \times [(K' + \lambda\phi_0^2)\sin^2(Q/2) - \lambda\phi_0^2] \end{aligned} \quad (14)$$

instead of (10). Therefore, for this model, the modulational instability does not depend on q , as for the continuum NLS equation. For $Q < Q^*$ determined by $\sin^2(Q^*/2) = \lambda\phi_0^2/(K' + \lambda\phi_0^2)$, all the carrier waves are unstable, while for $Q > Q^*$ they are stable.

As a consequence, for positive λ , the Ablowitz-Ladik model (13) can have localized modes either above or below the linear spectrum band (see, e.g., Refs. [24] and [25]). The comparison of the two models (4) and (13) shows thus that the *type* of discreteness has a major influence on nonlinear wave instability [26].

At last, we would like to mention that model (4) and the corresponding dispersion relation (10) can be considered a generalization of the results obtained from (1) by the semidiscrete approximation, well known in the theory of nonlinear discrete chains [13–16]. In this approach, the carrier wave is treated as discrete, but a continuum approximation is used for the envelope. Within such an approach, only long-wavelength modulation of the carrier can be investigated. Looking for solutions of Eq. (1) under the form

$$u_n(t) = \epsilon [F_1(n, t) e^{i\Theta_n} + \text{c.c.}] + \mathcal{O}(\epsilon^3), \quad (15)$$

where $\Theta_n = qn - \omega t$, ω and q being related by the linear dispersion relation (2), and expanding $F_1(n, t)$ versus the continuum variable x around site n , one gets the NLS equation

$$i \frac{\partial F_1}{\partial \tau} + P \frac{\partial^2 F_1}{\partial y^2} + G |F_1|^2 F_1 = 0 \quad (16)$$

in terms of the slow variables $y = \epsilon(x - V_g t)$ and $\tau = \epsilon^2 t$. Here, V_g is the group velocity of the wave, $V_g = (K/\omega)\sin q$, and $P = (K \cos q - V_g^2)/(2\omega)$, $G = 3\beta/(2\omega)$.

The stability of the plane-wave solution of Eq. (16) is determined by the following dispersion relation for the modulation waves:

$$(\omega_0 \Omega - KQ \sin q)^2 = \frac{1}{4} KQ^2 \cos q (KQ^2 \cos q - 6\beta\phi_0^2), \quad (17)$$

which gives the stability condition $PG < 0$. The dispersion relation (17) can be derived from Eq. (10) in the limit of small Q , i.e., in the long-wavelength limit for the modulation wave, which is assumed in the semidiscrete approximation.

III. NUMERICAL RESULTS

According to the analytical calculations presented above, the stability of a plane wave with wave number q modulated by a small-amplitude wave of wave number Q is determined by the dispersion relation (10). When the right-hand side of Eq. (10) is negative, we expect an exponential growth of the modulation. However, this

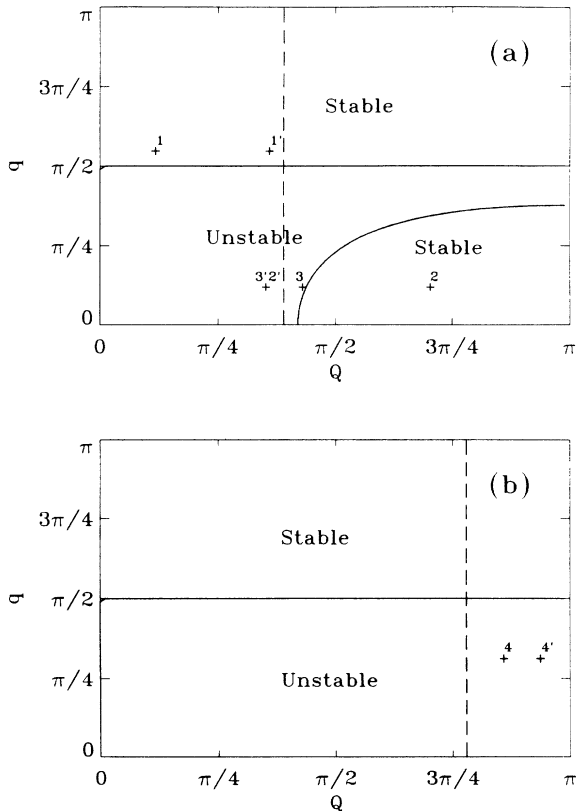


FIG. 2. Regions of modulational instability in the (q, Q) plane for $\beta > 0$, for (a) $\phi_0^2 < \phi_{0,cr}^2$ and (b) $\phi_0^2 > \phi_{0,cr}^2$. The points labeled by a number correspond to numerical simulations discussed in the text, and the dashed lines separate the regions of stability (large Q) and the regions of instability (small Q) as they would be determined by a formal application of the continuous NLS equation [Eq. (11)].

linear-stability analysis has been obtained through Eq. (4), which is only an approximate description of the initial equation (1). Moreover, the linear-stability analysis can only detect the onset of instability, but it does not tell us anything about the behavior of the system when the instability grows. In order to check the validity of our analytical approach and to determine the evolution of the system beyond the instability point, we have performed numerical simulations of the equations of motion (1). They have been integrated with a fourth-order Runge-Kutta scheme with a time step chosen to preserve the total energy of the system to an accuracy better than 10^{-4} over a complete run. The parameters of the model have been chosen to be $K=1$, $\beta=\pm 1$, and $\omega_0^2=100$, so that the condition $\omega_0^2 \gg 4K$ is satisfied. The initial condition is a modulated plane wave,

$$u_n(t) = (A + \alpha \cos Q) \cos(qn - \omega t).$$

Its amplitude A is related to the parameter ϕ_0 of the preceding section by $A=2\phi_0$, and the modulation amplitude is such that $\alpha \ll \phi_0$ ($\alpha=0.05$ for $\phi_0=0.5$ or 1.0). The simulations have been performed with a chain of $N=256$ units, with periodic boundary conditions so that the wave numbers q (Q) defined modulo 2π in a lattice, have to be chosen of the form $q=2p\pi/N$ ($Q=2P\pi/N$), where p (P) is an integer. The frequencies ω are deduced from the lattice dispersion relation (2).

As a first case, let us consider the case $\phi_0=0.5$, $q=1.7181$ ($p=70$), and a long-wavelength modulation $Q=0.3682$ ($P=15$) that corresponds to the point labeled by 1 in Fig. 2(a) displaying the stability regions in the (q, Q) plane for $\phi_0=0.5$. According to Fig. 2, we expect the modulated wave to be stable. The time evolution of the spatial Fourier components at wave numbers q and $q \pm Q$, which are present in the initial condition, is plotted in Fig. 3(a), which shows that the modulated wave is stable over the entire time range investigated (500 units of time, i.e., about 800 periods of a carrier at frequency $\omega_0=10$). As expected from the modulation-wave dispersion relation (10), the amplitude of the modulation oscillates in time. Figure 3(b) shows the time evolution of the complete spatial discrete Fourier transform of the displacements of the atoms in the chain,

$$s_p(t) = \sum_{n=0}^{N-1} u_n(t) e^{2i\pi pn/N} \quad \text{with } 0 \leq p \leq N/2. \quad (18)$$

In addition to the three main components contained in the initial condition shown in Fig. 3(a), Fig. 3(b) shows additional components at other wave numbers. They correspond to combination modes not included in the analysis, particularly the mode at wave number $3q$ that was neglected to derive Eq. (4) in the ‘‘rotating-wave’’ approximation, as well as combination waves at wave numbers $q \pm 2Q$. The time evolution of the amplitude of the wave number $3q$ is shown in Fig. 3(a). It oscillates in time, in agreement with the dispersion relation (10) applied to a wave of wave number q modulated by a small-amplitude wave of wave number $3q$. The corresponding point is the point labeled 1' in Fig. 2. It is in a stability region, since, for $q > \pi/2$, Eq. (10) indicates that the wave

is stable to *any* perturbation. This prediction of stability does not, however, guarantee that the wave will be permanently stable in the chain, because it neglects three-wave interactions. If the numerical simulation is carried on for about 4000 periods of the carrier wave, an instability finally shows up as the number of combination modes and their amplitudes increase. It should be noticed that the wave number Q of the initial modulation lies in a domain that would correspond to an unstable wave for

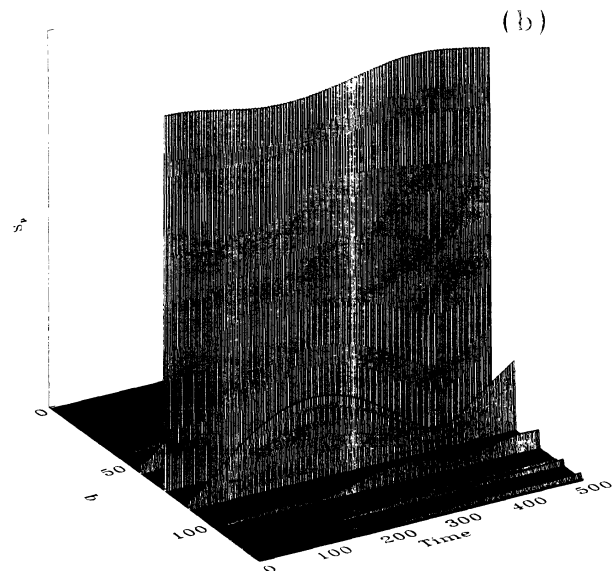
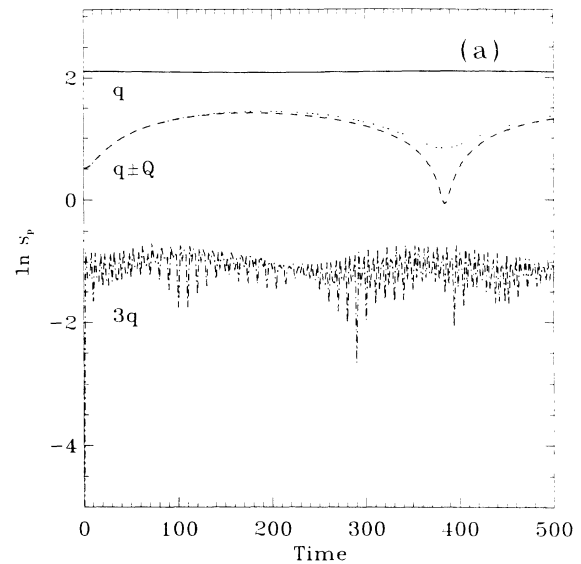


FIG. 3. (a) Time evolution of the Fourier components at wave number q (solid line), $q \pm Q$ (dotted and dashed lines), and $3q$ (dashed-dotted line) for a wave with amplitude $\phi_0=0.5$ and wave number $q=1.7181$ modulated at wave number $Q=0.3682$. Notice that the scale for the amplitude of the Fourier components is logarithmic. (b) Time evolution of the complete spatial Fourier spectrum of the wave.

the continuous NLS equation [Eq. (11)]. It is not surprising to find such a discrepancy because the wave of wave number $q=1.7181$ is indeed not correctly described by a continuum approximation.

Owing to the length of some of the simulations, it is important to check that the results are not affected by numerical accuracy. All the calculations have been performed with double-precision accuracy and, besides the check of energy conservation, we have verified the stability of the results with respect to a doubling of the time step. They are not modified by the change during the whole time evolution that precedes the chaotic regime, if it exists. When the chaotic regime is fully developed, the dynamics includes high-frequency modes, and the instantaneous positions and velocities of the particle observed at a given time are modified if the time step is doubled. It must be stressed, however, that the conclusion with respect to stability or instability is *not affected* by the change in time step because it is drawn from the results obtained before the chaotic regime shows up.

The numerical simulation discussed above simultaneously shows the strength and weakness of our analysis of the modulational instability in a discrete chain. On one hand, it gives a correct conclusion about stability, at least for a limited time, in a case where the conventional analysis based on the continuous NLS equation fails, but, on the other hand, since it ignores the combination modes generated by the nonlinear coupling, it is prone to errors. In order to analyze correctly the stability of a given wave, the simulation shows that we must not only consider the applied modulation Q , but also the $3q$ modulation arising from the nonlinear term. This method can be viewed as a first-order correction to the “rotating-wave” approximation used to derive Eq. (4). Its ability to detect a possible instability is illustrated by the following example. Let us consider a wave with $q=0.3682$ ($p=15$) modulated at wave number $Q=2.2089$ ($P=180$). The corresponding point in the (q, Q) plane in Fig. 2 (point labeled 2) lies in the stability region, whereas the point corresponding to $q-3q$ (point 2') is in the instability domain. Therefore, although the Q modulation is stable, we observe a spontaneous modulation arising from the $3q$ component that grows exponentially as shown in Fig. 4(a). The modulational instability is accompanied by a sharp increase of the maximum amplitude along the chain, from its initial value of $1.05(2\phi_0 + \alpha)$ to about 2.5, as shown in Fig. 4(b). Since the total energy of the system is conserved, this sharp rise in amplitude is associated with a localization of energy. The energy distribution, which was uniform in the initial wave, now exhibits large peaks at some sites.

This example shows that the analytical results leading to Eq. (10) give a correct estimation of the stability of a wave, provided that the combination modes, especially the mode of wave number $3q$, are taken into account. However, one must keep in mind that this analysis is only valid for a finite time because the nonlinear mode coupling finally takes over. The number of excited modes increases and the chain reaches a chaoticlike state in which all wavelengths are present. The transition to this chaoticlike state is sharp and associated with the sharp rise of

the maximum amplitude along the chain. Let us illustrate it by another case with $q=0.3682$ ($p=15$) as before, but $Q=1.3499$ ($P=110$). This case is interesting because the $q-Q$ point (point labeled 3 in Fig. 2) lies in the instability region very close to the border of the stability domain. Therefore, the behavior of the system tests the accuracy of our analytical approach. According to the stability analysis, we expect a weak instability of the Q modulation and a strong instability of the $3q$ modulation because the representative point (point 3' in Fig. 2, identi-

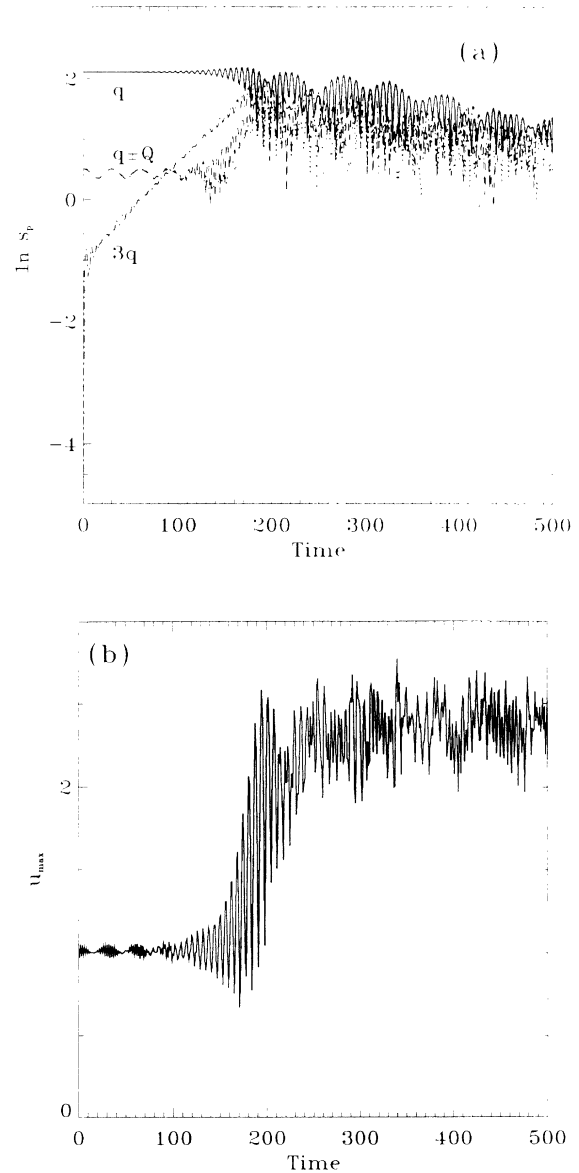


FIG. 4. (a) Time evolution of the Fourier components at wave number q (solid line), $q \pm Q$ (dotted and dashed lines), and $3q$ (dashed-dotted line) for a wave with amplitude $\phi_0=0.5$ and wave number $q=0.3682$ modulated at wave number $Q=2.2089$. Notice that the scale for the amplitude of the Fourier components is logarithmic. (b) Time evolution of the maximum amplitude along the chain.

cal to $2'$ as q is the same as in the previous case) lies well inside the instability region. This stability analysis is well confirmed by the numerical simulation as shown in Fig. 5(a), which displays the time evolution of the Fourier components of the Q and $3q$ modulations. The picture of the complete Fourier spectrum [Fig. 5(c)] shows the rather abrupt transition to a chaoticlike state, which is associated with the sharp rise in maximum amplitude along the chain observed in Fig. 5(b).

As a last example, let us consider the case of a larger amplitude, $\phi_0=1$. In this case, for $K=1$ and $\beta=1$, we expect that a wave with $q < \pi/2$ will be unstable against any modulation [see Fig. 2(b)]. This is illustrated in Fig.

6, obtained for $q=0.9817$ ($p=80$) and $Q=2.6998$ ($P=220$), which corresponds to points 4 ($q-Q$) and 4' ($q-3q$) in Fig. 2(b). For this higher amplitude the growth rate of the instability is high and a chaoticlike state is obtained after only 80 periods of the carrier wave. In this case, a stability analysis based on the continuous NLS equation [Eq. (11)] would predict stability for both the Q and $3q$ modulations, but owing to the large values of Q and $3q$ it is not surprising that an analysis based on a continuum approximation fails.

Our stability analysis is based on the discrete NLS equation (4) obtained with the assumption that ω_0^2 is large with respect to $4K$ and $\beta\phi_0^2$. It is interesting to check its

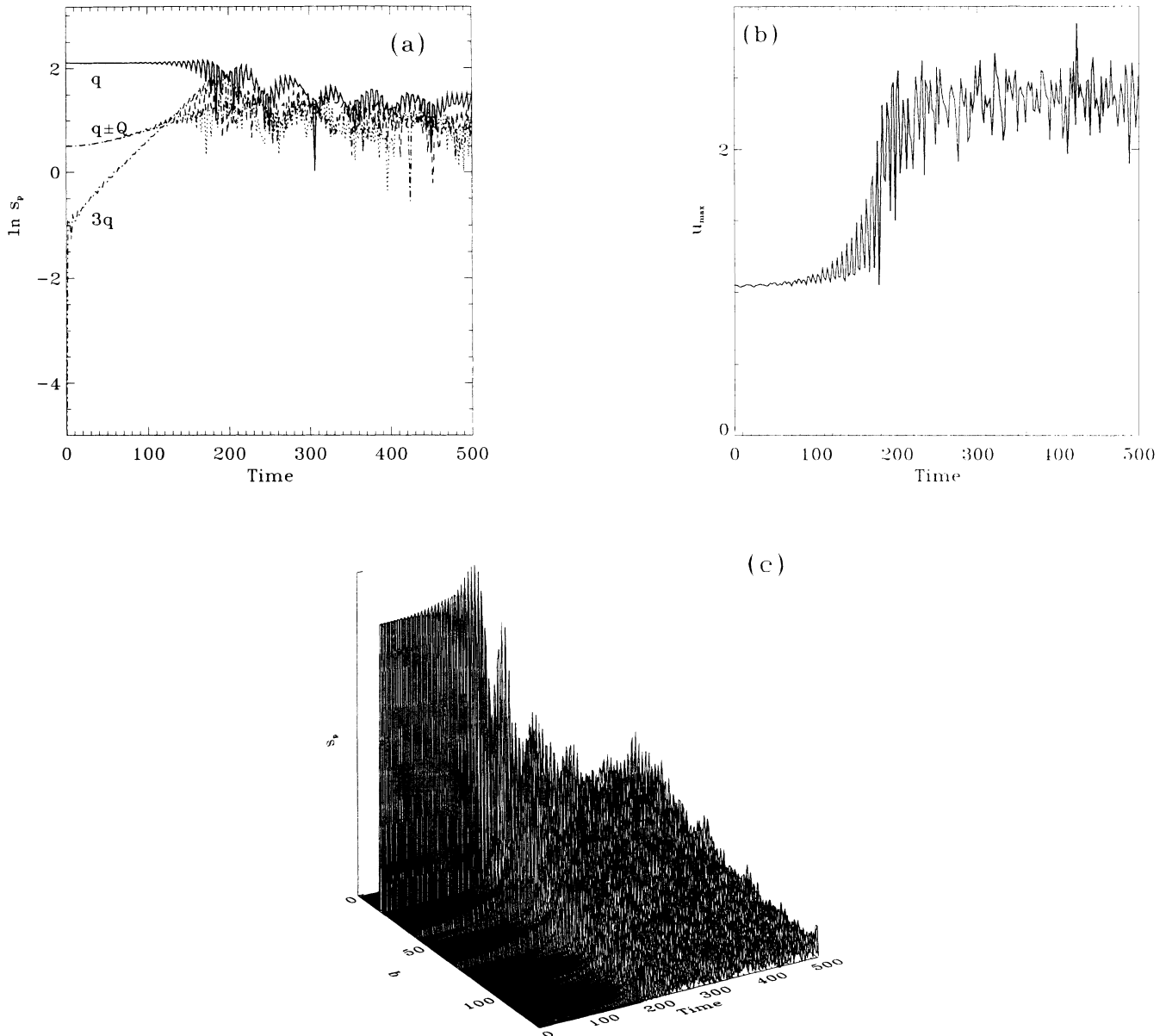


FIG. 5. (a) Time evolution of the Fourier components at wave number q (solid line), $q \pm Q$ (dotted and dashed lines), and $3q$ (dashed-dotted line) for a wave with amplitude $\phi_0=0.5$ and wave number $q=0.3682$ modulated at wave number $Q=1.3499$. Notice that the scale for the amplitude of the Fourier components is logarithmic. (b) Time evolution of the maximum amplitude along the chain. (c) Time evolution of the complete spatial Fourier spectrum of the wave.

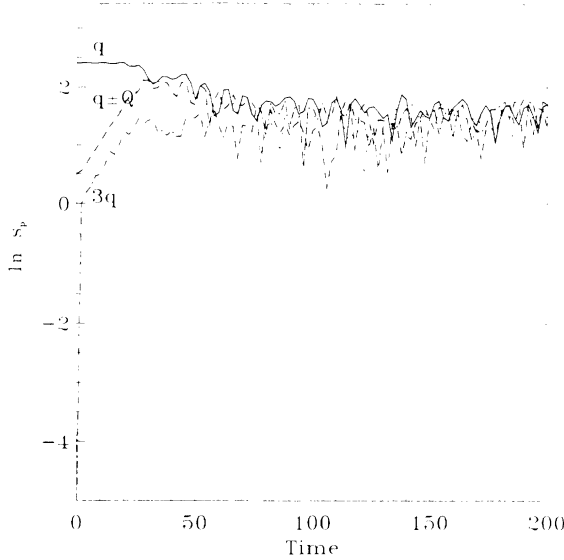


FIG. 6. Time evolution of the Fourier components at wave number q (solid line), $q \pm Q$ (dotted and dashed lines), and $3q$ (dashed-dotted line) for a wave with amplitude $\phi_0=1.0$ and wave number $q=0.9817$ modulated at wave number $Q=2.6998$. Notice that the scale for the amplitude of the Fourier components is logarithmic and that the time scale is not the same as in Figs. 3–5.

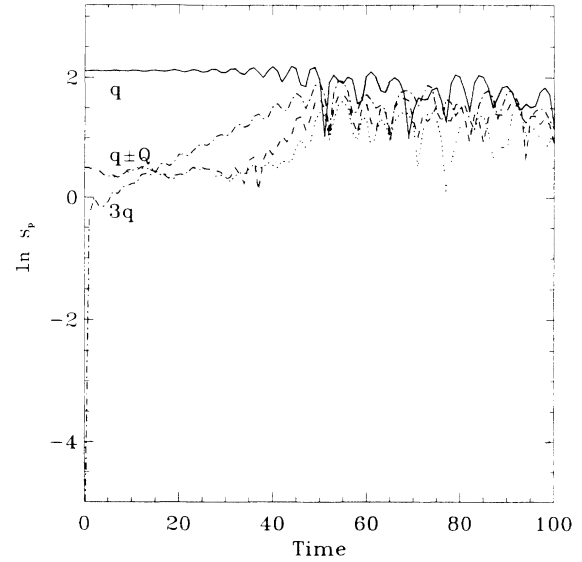


FIG. 7. Time evolution of the Fourier components at wave number q (solid line), $q \pm Q$ (dotted and dashed lines), and $3q$ (dashed-dotted line) for a wave with amplitude $\phi_0=0.5$ and wave number $q=1.7181$ modulated at wave number $Q=0.3682$. The parameters are the same as in Fig. 3, except for ω_0^2 , which has been reduced from 100 to 16. Note that the time scale is not the same as in Fig. 3.

validity for smaller values of ω_0 . Figure 7 shows the results of a numerical simulation performed with the same parameters as the one presented in Fig. 3, except for ω_0^2 , which has been reduced from 100 to 16. The parameters of the discrete NLS equation (4) are thus the same in both numerical experiments. Figure 7 shows that the initial evolution of the system is in agreement with the theoretical stability analysis. The Q modulation is stable while the $3q$ modulation is unstable, similar to the larger- ω_0 case. This shows that the condition of large ω_0 is not crucial for the analysis, but it is, however, important to determine the time after which the buildup of the combination modes will ruin the conclusions of the two-wave analysis. For $\omega_0^2=16$, the chaoticlike state mixing all wavelengths is obtained around $t=50$ units of time, instead of $t=200$ units of time for $\omega_0^2=100$.

IV. CONCLUSIONS

Our results, using the Klein-Gordon chain as an example, point out the crucial role of discreteness on modulational instability. First, the analytical approach based on a discrete NLS equation shows that the predicted stability domains are drastically modified with respect to the conventional results deduced from a continuum (or even semidiscrete) approximation. In particular, for a positive nonlinearity coefficient β , which is generally the relevant physical case as the potentials often soften for large amplitudes, a carrier wave at small wave numbers is unstable against all possible modulations when its amplitude exceeds a threshold.

The numerical simulations have confirmed the validity

of the theoretical analysis, provided that the stability is not only checked for the externally imposed Q modulation, but also for the $3q$ modulation generated by the nonlinear terms. However, they have also shown that stability can only be achieved for a limited time. The progressive build up of combination modes due to nonlinear coupling induces three-wave interactions that are not included in our analysis, and eventually all carrier waves evolve into a chaoticlike state where all possible wavelengths are present. In this state, the energy is no longer uniformly distributed along the chain, but, on the contrary, the amplitude of the motion of some particles becomes much larger than the amplitude of the original wave. Therefore, modulational instability in a discrete system appears to be a very efficient mechanism to generate large-amplitude solitonlike excitations. This is, for instance, the case in the discrete sine-Gordon model in which the formation of kinks (i.e., excitations with a amplitude of 2π) has been observed from the modulational instability of a plane wave of amplitude $\pi/3$ [27]. Since the small wave numbers show the largest growth rate, this explains why pulse or kinklike excitations ($q \approx 0$) rather than wave packets are easily generated by modulational instability in a discrete system.

The analytical results have also pointed out that the behavior of a nonlinear lattice depends strongly on the type of discreteness as shown by the differences found between our discrete NLS equation and the Ablowitz-Ladik integrable model. Our results can also be compared with the results obtained by Fermi, Pasta, and Ulam [28] on a chain with nonlinear coupling. They found that the equipartition of energy was extremely slow in the system,

while, for the Klein-Gordon lattice with on-site nonlinearity but an harmonic coupling, we observe that chaoticlike states mixing all the modes are easily obtained.

ACKNOWLEDGMENTS

Yu.K. thanks the Laboratoire Ondes et Structures Cohérentes for warm hospitality during his visit, when

this research work was initiated. He also acknowledges financial support from the Alexander von Humboldt Foundation during the final stage of this work. M.P. wants to thank the Center for Nonlinear Studies of the Los Alamos National Laboratory for hospitality and the Commission of the European Communities (CEC) for partial support of this work through Contract No. SCI-0705.

*On leave from Institute for Low Temperature Physics and Engineering of Ukrainian Academy of Sciences, 310 164 Kharkov, Ukraine.

- [1] G. B. Witham, Proc. R. Soc. London **283**, 238 (1965); J. Fluid Mech. **27**, 399 (1967).
- [2] T. B Benjamin and J. E. Feir, J. Fluid Mech. **27**, 417 (1967).
- [3] V. I. Bespalov and V. I. Talanov, Pis'ma Zh. Eksp. Teor. Fiz. **3**, 471 (1966) [JETP Lett. **3**, 307 (1966)].
- [4] V. I. Karpman, Pis'ma Zh. Eksp. Teor. Fiz. **6**, 759 (1967) [JETP Lett. **6**, 227 (1967)]; V. I. Karpman and E. M. Krushkal', Sov. Phys. Pis'ma Zh. Eksp. Teor. Fiz. **55**, 530 (1968) [JETP **28**, 277 (1969)].
- [5] L. A. Ostrovskii, Sov. Phys. Pis'ma Zh. Eksp. Teor. Fiz. **51**, 1189 (1966) [JETP **24**, 797 (1967)].
- [6] T. Taniuti and H. Washimi, Phys. Rev. Lett. **21**, 209 (1968).
- [7] A. Hasegawa, Phys. Rev. Lett. **24**, 1165 (1970); Phys. Fluids **15**, 870 (1971).
- [8] K. Tai, A. Hasegawa, and A. Tomita, Phys. Rev. Lett. **56**, 135 (1986).
- [9] K. Tai, A. Tomita, J. L. Jewell, and A. Hasegawa, Appl. Phys. Lett. **49**, 236 (1986).
- [10] M. Peyrard and A. R. Bishop, Phys. Rev. Lett. **62**, 2755 (1989); M. Peyrard, R. Boesch, and I. Kourakis, in *Collective Proton Transport in Hydrogen Bonded Systems*, Proceedings of the NATO Advanced Research Workshop, Heraklion, Crete, 1991, edited by T. Bountis (Plenum, New York, in press).
- [11] S. C. Lowell, Proc. R. Soc. London, Ser. A **318**, 93 (1970).
- [12] F. D. Tappert and C. M. Varma, Phys. Rev. Lett. **25**, 1108 (1970).
- [13] A. Tsurui, Prog. Theor. Phys. **48**, 1196 (1972); J. Phys. Soc. Jpn. **34**, 1462 (1973).
- [14] T. Kawahara, J. Phys. Soc. Jpn. **35**, 1537 (1973).
- [15] St. Pnevmatikos, M. Remoissenet, and N. Flytzanis, J. Phys. C. **16**, L305 (1983); **18**, 4603 (1985).
- [16] M. Remoissenet, Phys. Rev. B **33**, 2386 (1986).
- [17] J. L. Leroy, M. Kochoyan, T. Huynh-Dinh, and M. Guéron, Mol. Biol. **200**, 223 (1988).
- [18] A. J. Sievers and S. Takeno, Phys. Rev. Lett. **61**, 970 (1988).
- [19] S. Takeno, K. Kisoda, and A. J. Sievers, Prog. Theor. Phys. Suppl. **94**, 242 (1988).
- [20] V. M. Burlakov, S. A. Kiselev, and V. N. Pyrkov, Phys. Rev. B **42**, 4921 (1990).
- [21] K. Yoshimura and S. Watanabe, J. Phys. Soc. Jpn. **60**, 82 (1991).
- [22] Yu. S. Kivshar, Phys. Lett. A **161**, 80 (1991).
- [23] M. J. Ablowitz and J. F. Ladik, J. Math. Phys. **17**, 1011 (1976).
- [24] R. Scharf and A. R. Bishop, Phys. Rev. A **43**, 6535 (1991).
- [25] Yu. S. Kivshar (unpublished).
- [26] O. Kluth, Yu. S. Kivshar, K. H. Spatschek, and A. V. Zolotaryuk (unpublished).
- [27] M. Peyrard, T. Dauxois, and A. R. Bishop, in *Nonlinear Coherent Structures in Physical and Biological Systems*, edited by J. Leon (Springer-Verlag, Berlin, 1990).
- [28] E. Fermi, J. Pasta, and S. Ulam, in *The Collected Papers of Enrico Fermi* (University of Chicago Press, Chicago, 1965), Vol. 2, pp. 977-988.

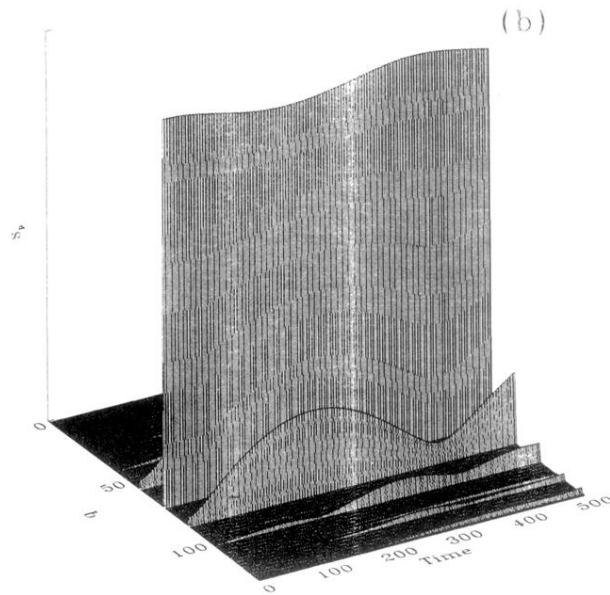
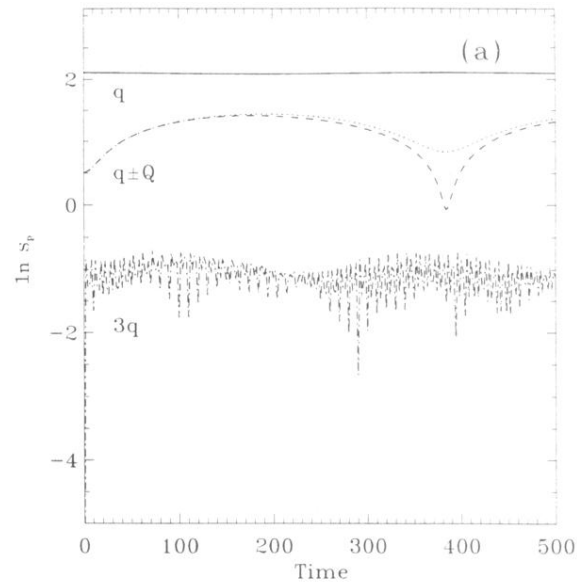


FIG. 3. (a) Time evolution of the Fourier components at wave number q (solid line), $q \pm Q$ (dotted and dashed lines), and $3q$ (dashed-dotted line) for a wave with amplitude $\phi_0=0.5$ and wave number $q=1.7181$ modulated at wave number $Q=0.3682$. Notice that the scale for the amplitude of the Fourier components is logarithmic. (b) Time evolution of the complete spatial Fourier spectrum of the wave.

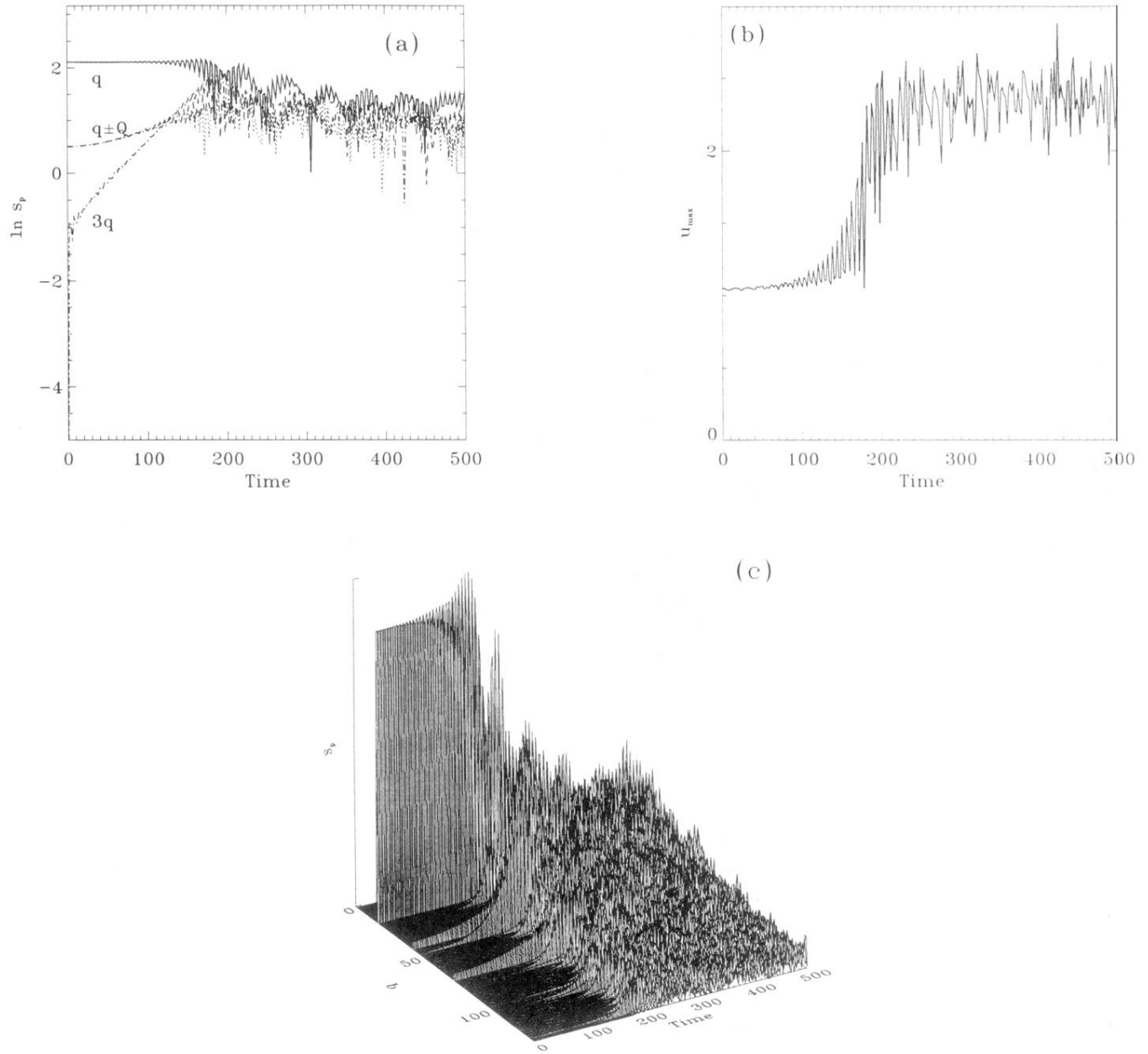


FIG. 5. (a) Time evolution of the Fourier components at wave number q (solid line), $q \pm Q$ (dotted and dashed lines), and $3q$ (dashed-dotted line) for a wave with amplitude $\phi_0=0.5$ and wave number $q=0.3682$ modulated at wave number $Q=1.3499$. Notice that the scale for the amplitude of the Fourier components is logarithmic. (b) Time evolution of the maximum amplitude along the chain. (c) Time evolution of the complete spatial Fourier spectrum of the wave.